Evaluation of particle settling in flow chamber

Abdulrahman Alenezi

Abstract – The investigation of fluids containing particles or filaments includes a category of complex fluids and is vital in both theory and application. The forecast of particle behaviours plays a significant role in the existing technology as well as future technology.

The present work focuses on the prediction of the particle behaviour through the investigation of the particle disentrainment from a pipe on a horizontal air stream. This allows for examining the influence of the particle physical properties on its behaviour when falling on horizontal air stream. This investigation was conducted on a device located at the University of Greenwich's Medway Campus. Two materials were selected to carry out this study: Salt and Glass Beads Nano particles. The shape of the Slat particles is cubic where the shape of the Glass Beads is almost spherical. The outcome from the experimental work were presented in terms of distance travelled by the particles according to their diameters as After that, the particles sizes were measured using Laser diffraction device and used to determine the drag coefficient and the settling velocity.

For a verification and more deep insight, the experimental setup was modelled using Computational Fluid Dynamics (CFD) technique and the results were compared with the experimental results in terms of distance travelled. A good agreement was observed between the CFD and experimental results.

The experimental and numerical results showed that the size of the particle has a huge impact on the drag coefficient and the settling velocity. Larger diameters lead to less drag and hence higher settling velocity. Also, the lighter particles tent to travel horizontally further than the heavier ones.

Acknowledgement – Thank you God for all your blessings to me and my family. For the strength you give me each day and for all the people around me who make life more meaningful. A teacher takes a hand, opens a mind and touches a heart. That is the definition of Dr. Zigan. All that I am or ever hope to be, I owe to my angel mother. My brother Ahmed, Thank you for always giving me the extra push I need.

Table of Contents

List of Figures

Nomenclature

A	surface area (m^2)
C_d	drag coefficient
C	Sutherland constant
d_p	particle diameter (m)
E	total energy (J)
$\overrightarrow{F}$	body force (N)
g	gravity (m/s^2)
G_{rs}	Archimedes number
$\dot{m}$	mass flow rate (kg/s)
P	pressure (Pa)
R	specific gas constant (J/kg.K)
Re_p	Reynold number
S_h	volumetric energy source term (J/m^3)
S_m	volumetric mass source term (kg/m^3)
t	time (s)
T	temperature (K)
$\vec{u}$	internal energy (J)
v	velocity (m/s)
V	volume (m^3)
$\dot{V}$	volume flow rate (m^3/s)
W_s	settling velocity (m/s)

Greek symbols

ρ	density (kg/m^3)
$\bar{\bar{\tau}}$	the stress tensor

Subscripts

f	fluid
p	particle

s	surface

Acronyms

CFD	Computational Fluid Dynamics
UTIAS	University of Toronto Institute for Aerospace Studies

1 Introduction

The investigation of fluids containing particles or filaments includes a class of complex fluids and is vital in both theory and application. Several studies have focused on the particle behaviour in a fluid flow. The forecast of particle behaviours plays a significant role in several engineering processes and fields, for example, chemical and metallurgical processes as well as mechanical and environmental engineering. Modelling of the particle in water process requires deep knowledge of predicting the particle velocity. In the gas turbine, blades and nozzles are exposed to erosion which is strongly rely on the particles velocities. A further application is the transmission of bulk material via pneumatic conveying, the assumption made for the particle motion is based on the terminal velocity of the particles. This emphasise the significance of predicting such velocity for selecting the right sizing and the appropriate design of the plant.

Regardless of such significance, the existing investigation do not offer a sufficient insight on such subject and enhancements of the prediction of the particles behaviours which in turns can lead to more accurate mathematical models. Also, the greater part of the existing studies is centred around the investigation of particles having regular shapes such as sphere (the least difficult and most researched shape), cubical or cylindrical shapes. Furthermore, the used material in these studies are fairly limited due to the irregular shape of their particles.

The present work focuses on the prediction of the particle behaviour through the investigation of the particle disentrainment from a horizontal air stream. The objective of the current study is to examine the effect of the particle properties on disentrainment on an air stream. The study was conducted using mechanical assembly which is located at the University of Greenwich's Medway Campus which is shown in Figure 1. Two different materials were considered in the current study, Salt, and Glass beads, were selected for their almost perfect spherical shapes. These experiments were repeat few times in order to verify the results and performances. Later on, the results were compared with the hand calculations and were further used to produce a two-dimensional Computational Fluid Dynamics (CFD) model.

2 Problem Statement

Today, the idea of particle granulomere has been liable to different sorts of research and concentrates instead of what it resembled 20 odd years prior. Researchers have acknowledged that issue comes in 3 unique states; strong, fluid and gas, frequently hidden the states in the middle. This order was handled by powders, which very still are solids, when circulated air through may carry on as fluids and when suspended in gas in may go up against a portion of the properties of gases. The expansion in innovation has made it conceivable to examine molecule conduct anyway there are insufficient gadgets to enable scientific models to foresee such attributes. For molecule measure investigation, granular materials are regularly utilized, which is known to be made of individual strong particles, paying little heed to its molecule estimate. Therefore, granular material can go from coarse colliery rubble to fine measured components.

Figure 1. Test apparatus.

3 Aim and objectives

The main goal of the current study is to investigate the particle interaction with air and the influence of particle properties such as particle size on the settling in a horizontal fluid flow. Another main goal of this study is to determine the drag coefficient of the particle.

To meet the aims, the objectives were defined as follows:

- Conduct a particle segregation experiment.
- Study various properties of particles and the effect of the fluid stream on the particle settling.
- Generate a CFD model to analyse the flow and to gain insight on the particles behaviour.

4 Literature Review

4.1 Introduction

Particle technology has already been adopted in a many formats and applications all over the globe throughout the history. Many kinds of powders have been produced to improve human life, such as food, detergents, pigments, cements, fertilizers and industrial chemicals.

Particle technology account to a significant contribution in many products, for instant, it contributes by almost one-half to the products within the chemical industry and over 75% of the granular raw materials [1].

In general, particle size can vary from sizes as small as order of nanometres up to 1 mm [2]. There is no general agreement on particle classification according its size is not, however, particles with less than 30 μm mean diameter are typically stated as fine particles which their uses in industries are huge. Particle having a diameter below 10 μm are referred to as superfine particles that can split down to: nanoparticles (1-100 nm) and molecular cluster (<1 nm), sub-micron particles (0.1-1 μm), micron particles (1-10 μm) [3].

4.2 Fluid-solid mixture

In the recent years, study of the mixture of fluid and fibres or particles gained an attention due to its importance to wide range of modern applications. The behaviour of particle in flow of fluid has been the focus of a large number of researches. One of the important behaviours of such particle is its velocities and trajectories as it plays a vital role in several engineering fields such as environmental and mechanical engineering besides chemical and metallurgical processes. The crucial problem is correlating the mixture properties at global level as well as local level. The existence of the solid particles in the fluid causes very complicated hydrodynamic phenomena [4-6].

There are two main forces acting on the settling particles as shown in Figure 2. First is the primary force such as gravity or forces due to centrifugal motion. Second force is the generated drag as a result of the particles motion in the fluid. The drag force is usually affected by the velocity of the particle where the applied force is not affected.

When the particle is not in motion, it will not experience any drag force and the particle will start to accelerate by means of the gravity force. After that, the drag force starts to act on the particle in the direction opposite to the motion. As the velocity of the particle build up, the drag force increases until it equates the applied force and the velocity of the particles will remain with no further change. This velocity referred to as settling velocity or terminal velocity of the particle.

There are many parameters that can alter the particle's terminal velocity. Any parameter affects the drag will directly affect the terminal velocity of the particle. Hence, the grain shape, size and density have the most effect on the terminal velocity in addition to the fluid properties.

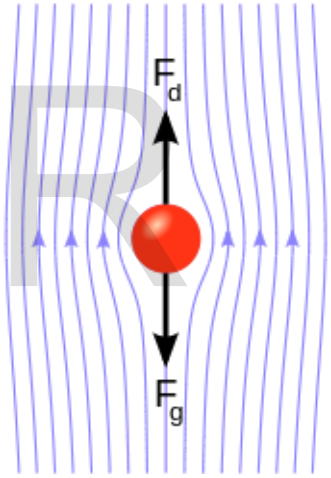

Figure 2. Flow over a settling sphere particle and forces acting on it [7].

In order to understand the natural phenomena of the mixture and various industrial processes, it is essential to determine the flow behaviour at local level as well as the potential interaction between the solid and liquid phases [8-12]. However, reviewing the available in the literature shows that studies been conducted to determine the global behaviour such as average concentration and velocity are relatively larger than the studies conducted to determine the local behaviour of the mixture. This shows that most of the studies are related to a specific application [13].

Using mass diffusion equations approach for modelling fluid flow provide approximation of the flow behaviour and in most cases, ignores some characteristics of the particles such as mechanical and physicochemical in

addition to the rheological behaviour of the mixture [14, 15].

In such situations, the terminal velocity of solid particles settling in fluid plays a significant role in the governing equations of such complex fluid flow [16-20]. Varity of relationships can be found to estimate the terminal velocity which makes it difficult to be applied [15, 21-23]. In the experimental investigations, a special interest is given to the effect of particle characteristics, such as density and shape, on sedimentation process [17, 24-29]. Also, the attention is paid to examine the effect of specific parameters of the fluid such as rheological characteristics and density [30-35].

The solid particles' terminal velocity is usually related to spherical shape. The proposed correlations for settling velocity are more likely to be implemented as a foundation for more complex shapes, which can be applied either directly or indirectly to evaluate the particle's setting velocity [36-39]. There are two methods to calculate the settling velocity of spherical particles. The direct approach treats the velocity as a function of dimensionless numbers roughly equivalent to an Archimedes number [40-45]. On the other hand, the indirect approach employs iterative process by using Reynold number and the drag coefficient [46-48] . By performing Bibliographic study, it was shown that the relationships are limited by small range of Reynold number [49, 50]. The validity of both theoretical and semi-theoretical treatments are limited to Reynold number less than unity.

4.3 Calculation methods of spherical particles settling velocity

When a particle settles in still fluid will accelerate for short period by means of gravity force until it reaches its terminal velocity, which occurs when the drag and gravitational forces are balanced. Therefore, the following relationship is obtained [51].

$$C_d = \frac{(\rho_p - \rho_f) g V}{\rho_f \left(\frac{W_s^2}{2}\right) A} \quad (1)$$

Where, V is the volume, A is the surface area, ρ_p is the particle density, ρ_f is the fluid density W_s is the settling velocity and C_d is the drag coefficient, which depend on Reynold number, Re_p, of the particle:

$$Re_p = \frac{d_p W_s}{g} \quad (2)$$

Where d_p is the diameter of the particle.

Practically, experimental data for terminal velocity along with W_s in Eqs. (1) and (2) t are usually used to generate the curve of $C_d=f(Re_s)$. While the conventional approaches use experimental data only to generate the curve $C_d=f(Re_s)$ and employ an iteration process to evaluate W_s. The curve $C_d=f(Re_s)$ have been described by several empirical correlations [12, 49, 52-56].

Also, there is possibility to use by direct calculation to calculate the value of settling velocity. In such instance, the parameters of Archimedes number, G_{rs}, should be taken into account. Hence, by altering Eq. (1) the following relationship can be obtained.

$$G_{rs} = \frac{(\rho_s - \rho_f) g d_p^3}{\rho_f \gamma^3} = \frac{3}{4} C_d Re_s^2$$

The value W_s for spherical particle can be obtained via $Re_s=h(G_{rs})$ along with Eq. (2) [40].

Most of the used relationships to determine the coefficient of drag are derived from data for settling velocity of particles in quiescent fluid. Other relationships were obtained for turbulent flow by placing a sphere in wind tunnel and measuring the drag coefficient [49]. It is worth noting that the value of the drag coefficient of sphere falling freely in static fluid is larger than when the surrounding fluid is in motion by 15-30%. The reason of this difference is that the when the particle falls in a quiescent fluid, its trajectory is more likely to be altered.

Despite that the relationships seems to singular for the Reynolds number and simple, other formulas have diverse and occasionally complicated [38]. However, all of these relationships share the same characteristic which expresses the hydrodynamic behaviour of the particle with its motion. There are three flow regimes that can categorise the hydrodynamic behaviour [14]:

- $Re_s < 1$: laminar.
- $1 < Re_s < 10^3$: transitional.
- $10^3 < Re_s < 10^5$: turbulent.

All the relationships show Stokes linearity but they don't have the same slope. Also, for the turbulent flow regime, the variation in the drag coefficient can be expressed as dependent on Re only.

The available relationships were proposed and adopted for both Newtonian and non-Newtonian fluids. This means the generalised Reynolds number was taken into account. Actually, the value of drag coefficient differs in both Newtonian and non-Newtonian fluids. In the flow regime having low Reynolds number, the drag coefficient for non-Newtonian fluid seems to be less than the value in Newtonian fluid case [32].

The literature review shows the models that adopt the direct calculation approach are more used to determine the drag coefficient than to determine the settling velocity. Majority of the drag coefficient models cover domains with wide range, which is sufficiently adapted to real-world applications.

5 Test apparatus

5.1 Chamber

The thought behind this work began from the perusing of the "Classification of solids particles in a horizontal air stream" report prepared by S.N. Farley-Hills, a student of Mechanical Engineering at the Thames Polytechnic of Woolwich. His work was cantered around the assessment and improvement of a current device at Thames Polytechnic. The mechanical assembly was a horizontal elutriator, i.e. equipment for the detachment of lighter and heavier particles in a two stage framework (i.e. gas-solids). Thusly, the Polytechnic had taken motivation from crafted by the University of Toronto Institute for Aerospace Studies (UTIAS). In the 1930's a few teachers of this University, built up a vertical section elutriator, called Infrasizer, which had some operational confinements, regarding the time required to embrace a trial and the level of accuracy for the mechanical assembly. In the 1997, they outlined a flat breeze burrow for the recreation of rain infiltration through an air stream, acknowledging later that they had manufactured an advancement of the Infrasizer, in view of an alternate physical rule. This new device was called Infrasizer Mark III and it allowed a superior part of the example in less time.

The device worked at 'The Wolfson Centre for Bulk Solid Handling Technology' depended on the plan found in the report 'Arrangement of strong particles in a level air stream'. Be that as it may, it was worked with another reason. The breeze burrow was produced at the Thames Polytechnic to get another instrument for molecule isolation, endeavouring to acquaint likewise an option with the utilization of strainers. Rather, The Wolfson Centre chose to utilize a similar mechanical assembly to examine the conduct of the particles in an airstream. Surely, one of the issues for the utilization of the contraption as an elutriator was the absence of learning of the streamlined parameters of particles with unpredictable shape. It was thusly chosen to switch the first technique: the breeze burrow was utilized to partition particles anticipating their arrival position by the utilization of numerical and physical demonstrating (a procedure influenced by the issue of a flawed information of particles conduct); now it is utilized precisely for a superior comprehension of this conduct, beginning from the arrival position of the particles in wind burrow floor. In this sense, the activity mode is the same in the two procedures, however the updated one required an exceptionally inside and out examination of the plate content after each test. This instrument has different sections. Table 1 shows the name of these sections and their measurements. Inside the working section there are 4 plates which will be explained later on the use of them. However, the dimensions of these plates will be shown in Table 2. Also, detailed drawing of the plate is shown in Figure 3.

Table 1. Main dimensions of the test apparatus.

Section name	Measurements (mm)
Pressure chamber	200 x 300 x 265
Working section	212 x 300 x 1370

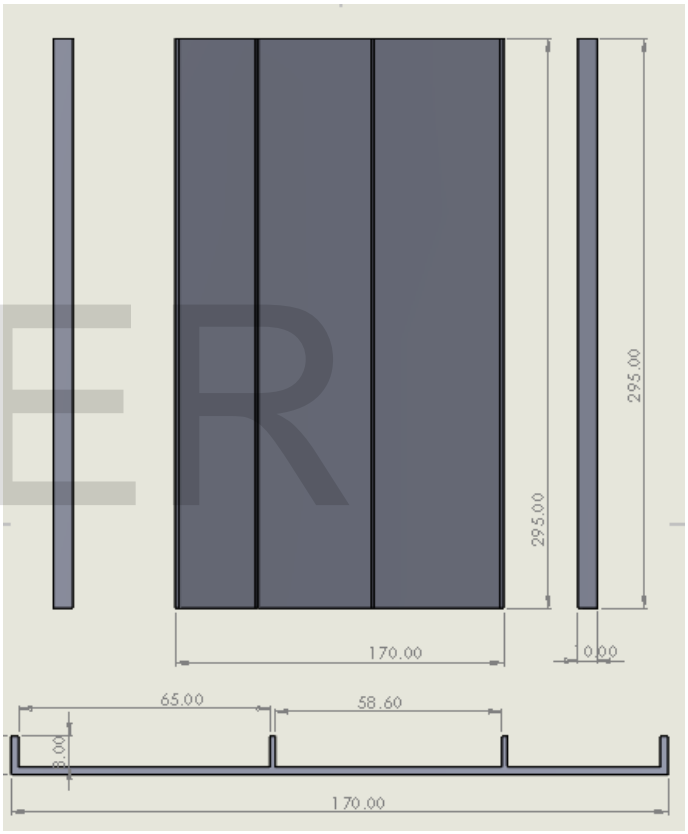

Figure 3. Plate drawing showing main dimensions.

Table 2. Working sections plates.

	Length (mm)	Width (mm)	Number of rows	Size of each row (mm)
Plate 1	170	295	8	20
Plate 2	200	295	8	25
Plate 3	500	295	10	
Plate 4	300	295	3	

5.2 Air delivering

The delivery of air is made by a blower CSD 102 of the Rotary Screw as shown in Figure 4. The air leaves the blower at a pressure of 6.8 bar and goes over a channel and a pressure reducer that declines the pressure to 5.2 bar. Now the air lands at the purported 'spout bank'. It is formed by an authority from which eight unique spouts begin. These spouts are controlled by on/off switches and have expanding opening areas. After the spouts, there is another gatherer associated with a progression of funnels that disseminate air in various parts of the research facility. The correct blend of spouts licenses to determinate a known conveying wind current rate.

Figure 4. CSD 102 air delivery unit.

5.3 Laser diffraction

The technique of laser diffraction depends on some physical standards which they found by Joseph von Fraunhofer. The diffraction is one of the impacts that happens when a lights hits a strong reflecting surface. For instance, if the light hits a molecule, its force diminishes because of the wonder of termination, caused by dispersing and ingestion. The main parts of the Laser diffraction s shown in Figure 5. The part of the light that isn't influenced by this, is called diffraction. The Fraunhofer diffraction considers the piece of the light being coordinated the forward way. The coming of the laser innovation, light touchy semiconductors of a sensible size joined with intense microcomputers have allowed the advancement of a specialized application for a quick and exact investigation of particles measure appropriation, in light of Fraunhofer's work. The Sympatec HELOS utilized for the examinations speaks to a case of this. In it, a laser pillar hits the particles to be examined. The range of the pillar diffracted is cantered by a focal point around a multi-component photograph detector The coming about picture 'read' by the identifier relies upon the number and size of the particles introduced in the estimating zone, and is changed over in an advanced flag meaningful from the PC. The example is perused as a conveyance of light forces and, through the use of a calculation; it is prepared utilizing a straight arrangement of conditions that closures with the assurance of the particles measure dispersion.

Figure 5. Laser diffraction device.

6 Experimental methodology

6.1 Preparation

6.1.1 Safety

Safety of the people in the laboratory comes first. Then safety of the equipment and other tools come later. So, the investigator must read and follow the laboratory instructions very carefully. The examiner must wear the safety clothes all the times while he /she in the laboratory. Which is in this case are (safety shoes, coat, and earplug each equipment in the laboratory has it been own safety procedure, so the investigator must be aware of it.

6.1.2 Setup

Firstly, the device full of dust not clean that will affect the result therefor must use the vacuum to clean it. The examiners hand is not long enough to reach the full chamber, so the examiner needed the aid of a piece of metal to accomplish the required job with aid of clippers. Then setting up the device get all the pieces of the device together and get it connected to the air control panel as it can be seen in Figure 6. This process is important to minimize the errors and to obtain an accurate result.

Figure 6. Chamber connected to the air control panel.

There is a hole in the top of the chamber. Using the pipe to fill the hole with the required material as it is shown in Figure 7. The material will be dropped freely. The air control panel will be on before dropping the material.

Figure 7. Preparation for the feeding.

The averge air velocity must be conisdered therefore must use a specific device which whill be in this case VOLTCRAFT (BL-30AN). This device is used to calculate the velocity of the air as it can be seen in Figure 8.

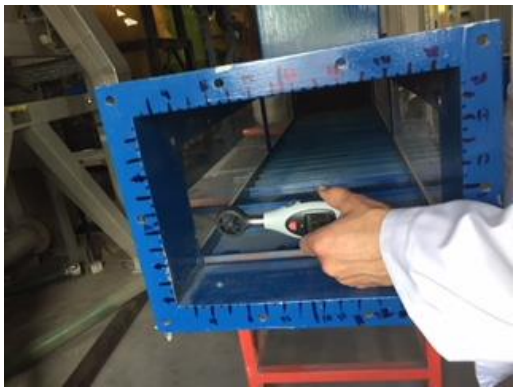

Figure 8. Air velocity measurement

Taking the average of the velocity of the air must be by repeating the experiment a few times. Figure 9 shows the locations of the measured places. Table 3 shows number of times that the experiment was repeated, the main reason for repeating it that to make sure of the values.

Location 1		Location 2
	Location 5	
Location 3		Location 4

Figure 9. Locations of the of air velocity measurements.

Table 3. Air velocity measurements.

Number of experiment	locations	Max velocity (m/s)	Average velocity (m/s)
1	1	0.90	0.15
	2	0.90	0.17
	3	0.90	0.17
	4	0.90	0.19
	5	0.90	0.17
2	1	0.90	0.15
	2	0.90	0.15
	3	0.90	0.15
	4	0.90	0.15
	5	0.90	0.15
3	1	0.90	0.11

	2	0.92	0.11
	3	0.92	0.11
	4	0.92	0.11
	5	0.92	0.11
4	1	0.92	0.11
	2	0.92	0.11
	3	0.92	0.11
	4	0.92	0.11
	5	0.92	0.11
5	1	0.92	0.11
	2	0.92	0.11
	3	0.92	0.11
	4	0.92	0.11
	5	0.92	0.11

After obtaining the numbers from the table must find the size of the chamber by using meter as shown in Figure 10 in order to calculate the volume flow rate of the air using Equations (4,5). The calculated value of the air flow rate are summarised in Table 4.

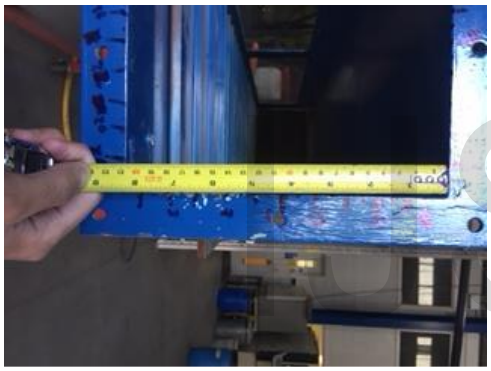

Figure 10. Finding the size of the chamber.

$$\dot{m} = \rho A v \quad (4)$$

where, $\dot{m}$ is the mass flow rate, ρ is the density, and v is the velocity. The volume flow rate can be calculated from the following equation:

$$\dot{V} = vA \quad (5)$$

Table 4. Air flow rate calculation results.

v (m/s)	$\dot{V}$ (m³/s)
0.11	0.0069
0.15	0.00945
0.17	0.01071

Since everything went ok now making the clean of the plates which they are 4 by using the brush as it can be seen in Figure 11.

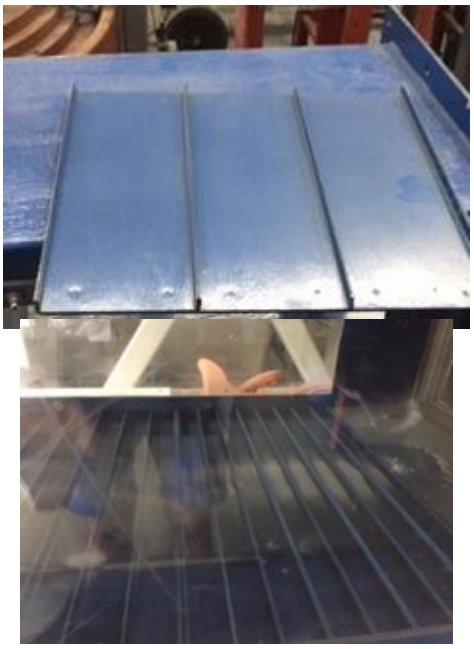

Figure 11. Cleaning the plats of the chamber

Then later using a specific tool for putting the Nano particle material into the pipe and the pipe must reach between 40 and 41 as it can be seen below in Figure 12.

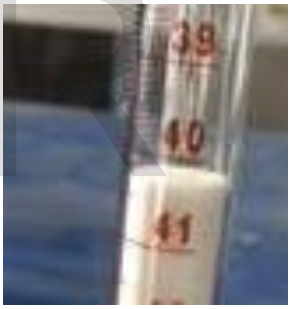

Figure 12. Filling the pipe with Nano particle material for injection.

The chamber is ready for the test and everything else is in the right position and ready to work.

6.2 Martials

6.2.1 Salt

Salt is a substance compound with various fascinating properties, precious stones or white crystalline powder, straightforward and dreary in crystalline shape, takes shape in the isometric framework, as a rule as blocks, solvent in water (35.6g/100g at 0°C and 39.2g/100g at 100°), marginally dissolvable in liquor, however insoluble in concentrated hydrochloric corrosive, melts at 801°C and starts to vaporize at temperatures only marginally over this breaking point 1,413°C, hardness of 2.5 on the MOH size of hardness, particular gravity of 2.165, non-flammable – low poisonous quality, hygroscopic – ingests

dampness from moist airs over 75 for each penny relative stickiness – beneath this, it will dry out. In its characteristic frame, salt frequently incorporates hints of magnesium chloride, magnesium sulfate, magnesium bromide, and others. These pollutions can tint the generally straightforward gems, yellow, red, blue or purple.

6.2.2 Glass beads

Glass beads have been broadly used to enhance the mechanical and warm properties of business polymers. In the previous couple of decades there have been numerous reports of examinations identified that is regarding of this subject. It has diameter of 4.0 μm, it has elasticity of 10.0 psi, and density of 2500 kg/m^3.

6.2.3 Air properties

The conduct of a molecule in a liquid relies upon numerous factors. Thus, is critical to have a decent learning of the different performers of this communication. The imperative qualities of the particles are its thickness, volume and shape while for the liquid are its physical properties of thickness and dynamic consistency.

6.2.3.1 Density

The air properties are impacted by the warm normal for temperature and weight. A simple method to portray the connection between these properties is the utilization of the state condition for perfect gas:

$$\frac{P}{\rho} = RT \tag{6}$$

where, T is the air temperature, R is the air specific gas constant, P is the pressure, and ρ is the air density.

Regardless of whether air isn't a perfect gas, it can be dealt with as it when the weight accepts low esteem (p → 0). For expanding weight esteem, a variety of gas conduct happens. To express this hole is utilized a factor Z, characterized as p/ (ϱ RT), that accept 1 as incentive for the perfect gas. This factor diminishes with expanding weight, and bad habit versa increments with expanding temperature. Be that as it may, it expects applicable qualities just for high estimations of weight. Our work lord conditions are: air weight (101325 Pa) and a temperature of around 16 °C. In this condition, the hole of the factor Z is under 0.5% and along these lines air can be considered as a perfect gas furthermore, the condition can be utilized without significant blunder.

6.2.3.2 Viscosity

In the past section, it was clarified that the working condition allow to sell out the air as a perfect gas. In the legitimacy field of the condition the dynamic consistency depends just in the temperature and it is almost autonomous of the weight. The reliance of consistency on temperature is communicated by Sutherland's condition:

$$\mu = \mu_o \sqrt{\frac{T}{T_o}} \cdot \frac{1 + \frac{C}{T_o}}{1 + \frac{C}{T}}$$

where μ is the dynamic viscosity, μ_o is the dynamic viscosity at $T_o = 0$ °C which has a value of 1.72 x 10^{-5} N.s/m ^{2} for air, and C is the Sutherland constant which is considered to have a value of 113 K. the value of T is assumed to be 289.13 K.

6.3 Experiment

6.3.1 Assumption

6.3.1.1 Acceleration

In the model it was disregarded the increasing speed length of particles while entering in the working segment. Notwithstanding, the molecule section conditions are not totally known. In the pipette last tract, particles started their speeding up vertical way however the speed came to before leaving the pipette was not contemplated and it is not correct to accept that it was equivalent to the maximum speed in a limitless liquid.

6.3.1.2 Interaction of the particles

The numerical model was made for a detached molecule in an air stream. Be that as it may, regardless of whether it was attempted to have a low molecule stream rate on account of the presentation of the pipette as encouraging gadget, the particles entered noticeable all around stream in considerable numbers (giving extent of between molecule activities). Numerous marvels can occur that may add to a randomisation of the settling conduct and subsequently the last area on the floor of the particles. Particle crash: the distinctions in estimate between particles prompts a distinction in the falling speed. In this manner it could happen, particularly toward the start of their movement where particles of various size are still in closeness to each other, that a quicker molecule could crash into a slower moving one. The outcome is a trade of energy that rates up the slower molecule while it diminishes the speed of the quicker one. Particle amassing: it could happen that some surface powers between particles emerge, due for instance to erosion or electrostatic impact. At the point when this marvel happens, at least two particles will act like a one of a kind greater molecule, achieving a max speed higher than anticipated. Aerodynamic connection: the wake left noticeable all around stream by particles could meddle in the falling of following particles. For instance, if a little dot enters the wake of a bigger one, it will take after another direction, expecting a higher falling velocity. Gravitational power: it is likewise possible that, if the distinction in estimate between two particles is exceptionally significant, a major molecule will pull in

gravitationally a minor molecule, which will act as a satellite in regard of the biggest. Every one of these sorts of association will likely adjust the molecule conduct inside the passage, particularly the one of littlest particles. Specifically, it was normal the nearness inside the plate of a small amount of particles littler than gauge by the two conditions.

6.3.1.3 Behaviour of the air

The wind current inside the passage was subject of broad examination amid the improvement of the test technique. The primer tests embraced, had shown that the stream was straight and uniform in the region assigned for particles falling. Be that as it may, the examination was confined to a few territories of the passage where the passage adaptation allowed it. Consequently, the air conduct was not totally known and could (conceivably) produce unforeseen wonders such, as turbulences or bearing possibilities. Specifically, the inward state of the plate expands the likelihood of the nearness of air recirculation along the passage floor. This perspective, or others not considered here, could randomize the particles movement and thus their last arrival position.

6.3.2 Testing

After doing all these steps the chamber is ready for establish the experiment. This experiment is separated into two main parts. Each part has a specific goal. Then, adding up these steps to end up with the results of this experiment.

6.3.2.1 Part 1

The main target of this part is testing the flow of two Nano particle materials (salt, and glass beads) by dropping them separately from a hall in the chamber while the air flow is going on. Then, collecting the samples and the data from the chamber. This chamber has many plates. Each plate has number of rows. So, the examiner followed the instruction of the supervisor by collecting data from every three rows as one tray by using the brush as it can be seen in Figure 13. Lastly use the bags to be filled of the samples. After that the vacuum used again to clean the lab and get back every tool that has been used to it is place.

Figure 13. Particle collection using fine brush.

6.3.2.2 Part 2

This part is taking the samples that were obtain in part one. First step in this part is taking the measurement of the samples all by using the scale as it can be seen in the Figure 14 below. This step is important because it will help to pick out the efficient results and eliminate or neglect inefficient results.

Figure 14. Using the scale for getting the measurement

Table 5 shows salt test results, the number of experiments which it were three in this case. Each experiment has two bags as a result of the experiment. The first bag was for tray 1 (1-3) and the second bag was for tray 2 (4-6). However, bag 2 is neglected for all of the Salt experiments as it has very small quantity of particles.

Table 5. Salt test results.

Test	Bag	Weight (mg)	Particle size distance measurement
1	1	16619	Measured

	2	861	Not Measured because it is not enough (quantity)
2	1	17100	Measured
	2	1247	Not Measured because it is not enough (quantity)
3	1	15886	Measured
	2	743	Not Measured because it is not enough (quantity)

Table 6 shows Glass beads test results, the number of experiments which it was 3 in this case. Each experiment has three bags as a result of the experiment. The first bag was for tray 1 (1-3), the second bag was for tray 2 (4-6), and the third bag was for tray 3(7-9).

Table 6. Glass beads test results.

Test	Bag	Weight (mg)	Particle size distance measurement
1	1	11767	Measured
	2	7152	Measured
	3	2438	Measured
2	1	11829	Measured
	2	7255	Measured
	3	2064	Measured
3	1	11375	Measured
	2	7129	Measured
	3	2460	Measured

Again, to start this experiment must clean the laboratory before getting started by using the vacuum cleaner. Must turn on the computer first because it is connected to it. Otherwise doing the experiment is useless. Then turn on the air flow key. Lastly turn the laser machine on as it can be seen in Figure 5.

7 Result &Discussion

7.1 Experimental results

7.1.1 Salt results

As it can be seen in Figure 15 that the salt test result was shown by trays. There were 3 experiments, and all these experiments were attempted in the first tray (1-3) due to the lack of quantity of the Nano particle material (Salt). The experiments from 1-3 showed results 267, 266, and 265 μm respectively. The average of this was calculated 266 μm. The distance travelled result for tray (1-3) is 65 mm.

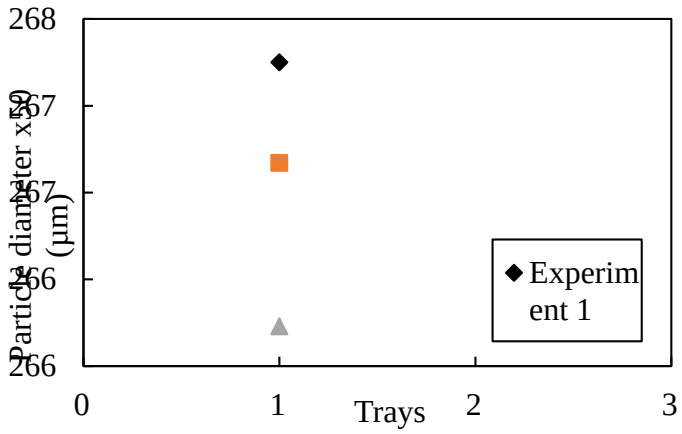

Figure 15. Salt test results by trays for experiment 1.

7.1.2 Glass beads results

As it can be seen in the figure 14 the glass beads test result was shown by experiment. There were 3 experiments, and all these experiments were attempted in the trays (1-3), (4-6), and (7-9). The experiment 1 showed result 121, 121, and 122 μm respectively. The experiment 2 showed result 118, 118, and 119 μm respectively. The experiment 3 showed result 124, 124, and 124 μm respectively. The average for tray (1-3), (4-6), and (7-9) is 121, 121, and 122 μm respectively. The distance travelled result for trays (1-3), (4-6), and (7-9) are 65, 125, and 195 mm respectively.

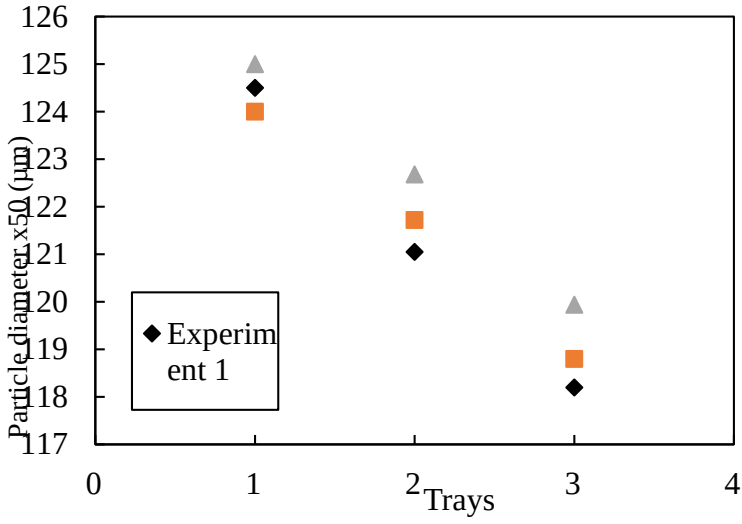

Figure 16. Glass beads results by trays

Salt test has a bag for each experiment, and Glass beads test has 3 bags for each experiment because of the proprieties of the Nano particle material. Therefore, it will absolutely affect the particle size distance measurement.

7.2 Hand calculation results

Table 7 shows the hand calculations of drag coefficient (C_d) of the each tray of the Salt and Glass beads. Which supports the experimental results. An important factor in this calculation was the behaviour of this experiment was laminar. It was found after calculating the Reynold number (Re) for each tray must have calculated a few things such as distance travelled of the particle size, density of Nano particle materials (Salt, and Glass beads), volume flow rate of particle (V), settling velocity (W_s), area of Nano particle materials (Salt, and Glass beads), diameter of Nano particle materials (Salt, and Glass beads) (d_p), and viscosity of Nano particle materials (Salt, and Glass beads) (μ). It is clear that the drag coefficient in tray 1 is bigger than tray 2, and the drag coefficient in tray 2 is bigger than tray 3. And the main reason for that is the diameter. The relationship will be explained further in Figure 17 and Figure 18.

Table 7. Hand Calculation.

	Tray	Distance (mm)	ρ_p (kg/m^3)	ρ_f (kg/m^3)	V (m^3)	Ws (m/s)	A (m^2)	Re	d_p (μm)	μ (N.S/m^2)	C_d
Salt	1	65	2160	1.22	1.89381E-11	4.65	4.26E-07	1.26E-04	267	1.7995E-05	0.071
	1	65	2500	1.22	1.01E-12	1.17	4.9E-08	1.5E-05	125	1.7995E-05	0.605
Glass	2	125	2500	1.22	9.461E-13	1.12	4.7E-08	1.4E-05	122	1.7995E-05	0.647
	3	195	2500	1.22	8.823E-13	1.07	4.4E-08	1.3E-05	119	1.7995E-05	0.693

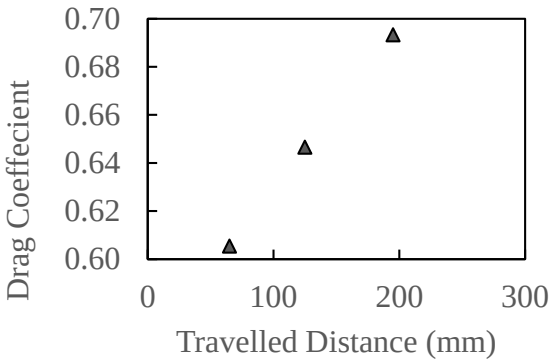

Figure 17. Drag coefficient of the particles against the travelled distance.

Figure 17 shows the drag coefficient decreasing against distance and that because of motion resistance. So in overall the drag coefficient has an inverse relationship with distance. This is the result of Glass beads. For tray 1 travelled distance is 65mm, tray 2 travelled distance is 125mm, and tray 3 travelled distance is 195mm.

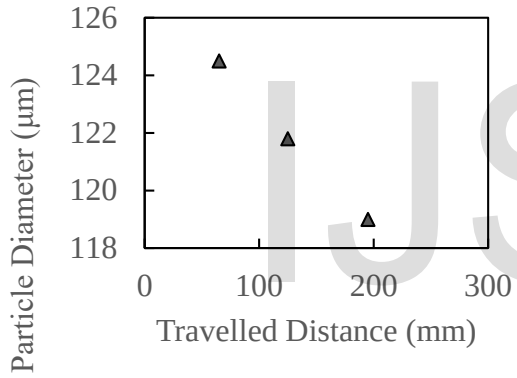

Figure 18. Particle diameter against distance travelled.

When the diameter increases the drag coefficient decrease. So when the diameter increase the distance will increase as well. For tray 1 diameter is 1.25E+02, tray 2 diameter is 1.22E+02, and tray 3 diameter is1.19E+02, Therefore, there is a proportional relationship as it can be seen in Figure 18.

7.3 CFD modelling

7.3.1 Methodology

Two - dimensional calculations were conducted using the CFD software of ANSYS FLUENT. The general methodology is well established and can found in many text books such as Versteeg et al. [57]. This technique based on solving Navier-Stokes equations beside continuity and energy equations within the computational grid.

In the CFD code ANSYS Fluent, the governing differential equations is formulated using the finite volume approach. Three conservation laws of physics are representing the governing equations of the fluid flow as follow:

- *Mass conservation*

  By applying the mass conservation principle on a control volume, the continuity equation can be written as [58]:

$$\frac{\partial \rho}{\partial t} + \nabla.(\rho\overrightarrow{v}) = S_m \tag{8}$$

where $\overrightarrow{v}$ is the velocity, ρ is the fluid density, and S_m is the mass source term. This equation is is valid for both incompressible and compressible flows while the first term becomes zero, $\frac{\partial \rho}{\partial t} = 0$ for incompressible flow

- *Momentum conservation*

  By applying Newton's second law on an infinitesimal control volume, the momentum equation can be written as [58]:

$$\frac{\partial}{\partial t}(\rho\overrightarrow{v}) + \nabla.(\rho\overrightarrow{v}\,\overrightarrow{v}) = -\nabla p + \nabla.(\bar{\bar{\tau}}) + \rho\overrightarrow{g} + \overrightarrow{F} \tag{9}$$

  where $\overrightarrow{F}$ and $\rho\overrightarrow{g}$ are the external body force and the gravitational body force and e, $\bar{\bar{\tau}}$ is the stress tensor and p is the static pressure.

- *Energy conservation*

  the energy equation can be derived by applying the first law of thermodynamics on a control volume to and can be expressed as [58]:

$$\begin{aligned}\frac{\partial}{\partial t}(\rho E) + \nabla.\left(\vec{u}(\rho E + p)\right) \\ = -\nabla.\left[k_{eff}\nabla T - \sum_j h_j\vec{J}_j \right. \\ \left. + \left(\bar{\bar{\tau}}_{eff}.\vec{u}\right)\right] + S_h\end{aligned} \tag{7.1}$$

  where E is the total energy, k_{eff} is the effective thermal conductivity, and S_h the heat source term and $\vec{J}_j$ is diffusion flux of species j.

The Reynold numbers at the chamber inlet and around the particle are small enough to consider the flow regime to be laminar. Gravity is activated to take into account the

buoyancy forces acting on the particles. After trying several meshes, the grid was selected with about t 25,000 cells as shown in Figure 20.

The boundary conditions at the chamber inlet is considered as velocity inlet with magnitude of 0.11 m/s where at the exit side pressure outlet condition is applied. In addition, no slip wall boundary conditions is imposed at all of the other outer surfaces and at the trays with its spacers. The particles are injected from a location on the top of the chamber as show in Figure 20. In order to model the interaction between the air stream and the injected particles, Discrete Phase Model (DPM) is implemented. The Rosin-rammler model is chosen to take into account the variations in the particles sizes, which varies from 10^{-5} to 10^{-4} according to the experimental results. In the current model, the used particle material is Glass beads with constant density of 2500 kg/m^3. Also, the air density is assumed to be constant throughout the calculations with value of 1.22 kg/m^3.

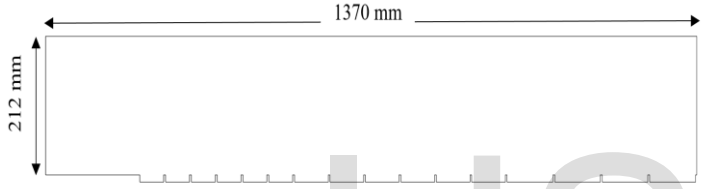

Figure 19. 2-D sketch of the geometry used in CFD model.

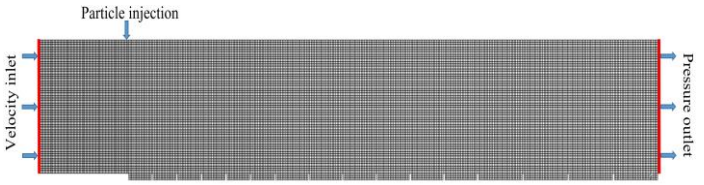

Figure 20. Computational grid and boundary conditions

7.3.2 CFD modelling results

Figure 21. shows the air velocity distribution within the chamber. The air boundary layer near to the wall is very obvious form this figure, where the velocity at the wall is zero and increases toward the centre of the chamber.

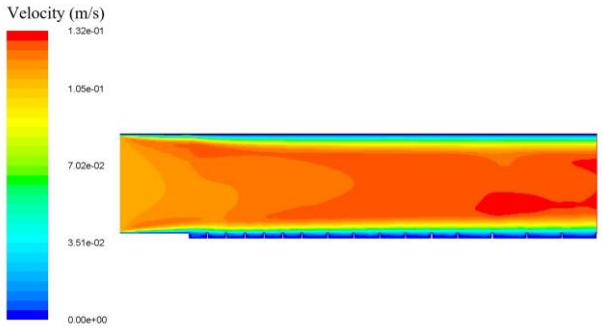

Figure 21. Air velocity contour.

Figure 22 shows the particle distribution within the chamber section. It can be clearly seen that the particles with large diameter falls first where the particles with smaller diameters falls later. This also agrees with the experimental results.

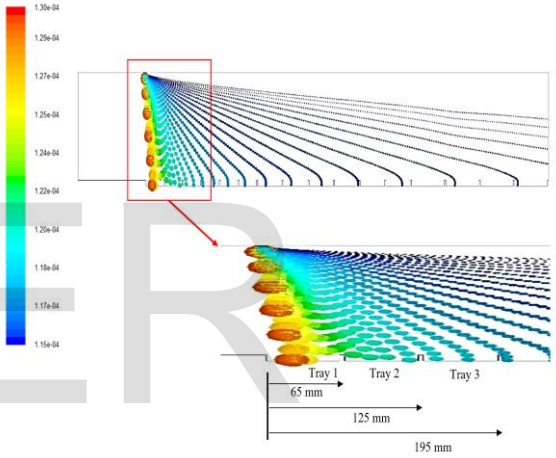

Figure 22. Particle tracking coloured by the particle diameters.

A comparison between the experimental results and the CFD results is shown in Figure 23 in terms of the distance travelled by the particle according to their diameters. A general agreement can be seen between the experimental and CFD results. However, the diameter size of the particles descended in the first tray are relatively over estimated by the CFD, while the diameter size dropped in the other trays are slightly underestimated. This is may be due to neglecting the 3D nature of the process and reducing it to 2D.

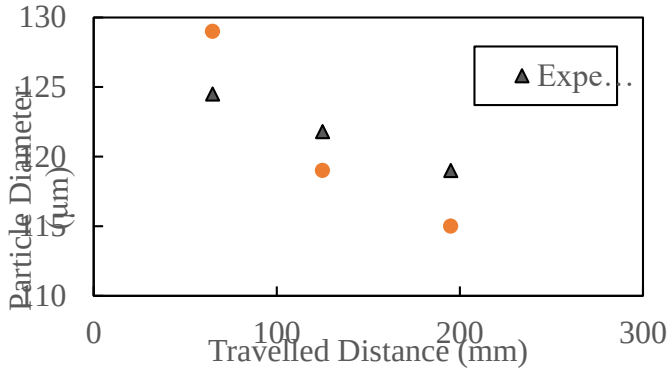

Figure 23. Comparison between experimental results and CFD results.

8 Conclusion

The experiment was successfully performed to examine the particles behaviours. The effect of the particles physical properties on its behaviours within a flow of air stream was examined. A CFD model was generated to verify the experimental results and to provide deep insight of the behaviours of such particles. A good agreement was found between the CFD model results and the experimental results.

It was found from both experimental and numerical results that the size and shape of the particle has a huge impact on the drag coefficient and the settling velocity. Particles with larger diameters tent to experience less drag force and hence this lead to higher settling velocity. Also, the lighter particles tent to travel horizontally further than the heavier ones.

9 Future work& Recommendations

There are few things can be done in the future to improve the understanding of the particle behaviours such as:

- Consider a different shapes of particles.
- Replicate the experiment at different air velocities to allow the heavy Salt particles to spread further.
- In this work the flow regime was laminar, in the future the experiment can be conducted for turbulent flow regime to provide more understanding of the particles behaviour in such flow.

References

[1] R. M. Nedderman, *Statics and kinematics of granular materials*: Cambridge University Press, 2005.

[2] Y. Arai, *Chemistry of powder production* vol. 6: Springer Science & Business Media, 2012.

[3] N. Ichinose, Y. Ozaki, and S. Kashu, *Superfine particle technology*: Springer Science & Business Media, 2012.

[4] J. M. DallaValle, *Micrometrics: The technology of fine particles*: Pitman, 1948.

[5] W. H. Graf, *Hydraulics of sediment transport*: Water Resources Publication, 1984.

[6] V. L. Streeter, E. B. Wylie, and K. W. Bedford, "Fluid mechanics, WCB," ed: McGraw-Hill, 1998.

[7] G. K. Batchelor, *An introduction to fluid dynamics*: Cambridge university press, 2000.

[8] L. C. Van Rijn, *Principles of sediment transport in rivers, estuaries and coastal seas* vol. 1006: Aqua publications Amsterdam, 1993.

[9] J. Baba and P. D. Komar, "Measurements and analysis of settling velocities of natural quartz sand grains," *Journal of Sedimentary Research*, vol. 51, 1981.

[10] D. M. Burr, J. P. Emery, R. D. Lorenz, G. C. Collins, and P. A. Carling, "Sediment transport by liquid surficial flow: Application to Titan," *Icarus*, vol. 181, pp. 235-242, 2006.

[11] E. Mendoza and R. Silva, "Physical characterizations of sands and their influence in fall velocity," *American Journal of Environmental Sciences*, vol. 4, pp. 238-244, 2008.

[12] R. Clift, J. R. Grace, and M. E. Weber, *Bubbles, drops, and particles*: Courier Corporation, 2005.

[13] A. Fortier, *Mechanics of suspensions*: Masson et Cie, 1967.

[14] F. M. White, "Fluid mechanics. 5th," *Boston: McGraw-Hill Book Company*, 2003.

[15] E. Michaelides and B. Particles, "Drops: Their Motion," *Heat and Mass Transfer, World Scientific, Singapore*, pp. 23-156, 2006.

[16] H. Schlichting and K. Gersten, *Boundary-layer theory*: Springer, 2016.

[17] N. Hawley, "Settling velocity distribution of natural aggregates," *Journal of Geophysical Research: Oceans*, vol. 87, pp. 9489-9498, 1982.

[18] R. Soulsby, *Dynamics of marine sands: a manual for practical applications*: Thomas Telford, 1997.

[19] J. P. Ahrens, "A fall-velocity equation," *Journal of waterway, port, coastal, and ocean engineering*, vol. 126, pp. 99-102, 2000.

[20] H. Gan, J. J. Feng, and H. H. Hu, "Simulation of the sedimentation of melting solid particles," *International journal of multiphase flow*, vol. 29, pp. 751-769, 2003.

[21] K. Heiskanen, *Particle classification*: Chapman & Hall London, 1993.

[22] P. P. Brown and D. F. Lawler, "Sphere drag and settling velocity revisited," *Journal of Environmental Engineering,* vol. 129, pp. 222-231, 2003.

[23] R. P. Chhabra, *Bubbles, drops, and particles in non-Newtonian fluids*: CRC press, 2006.

[24] R. J. Gibbs, M. D. Matthews, and D. A. Link, "The relationship between sphere size and settling velocity," *Journal of Sedimentary Research,* vol. 41, pp. 7-18, 1971.

[25] S.-F. Chien, "Settling velocity of irregularly shaped particles," *SPE Drilling & Completion,* vol. 9, pp. 281-289, 1994.

[26] H. Hofmann, "Grain-shape indices and isometric graphs," *Journal of Sedimentary Research,* vol. 64, 1994.

[27] J. Le Roux, "Comparison of sphericity indices as related to the hydraulic equivalence of settling grains," *Journal of Sedimentary Research,* vol. 67, 1997.

[28] P. Tang, H.-K. Chan, and J. A. Raper, "Prediction of aerodynamic diameter of particles with rough surfaces," *Powder technology,* vol. 147, pp. 64-78, 2004.

[29] N. Agarwal and R. Chhabra, "Settling velocity of cubes in Newtonian and power law liquids," *Powder Technology,* vol. 178, pp. 17-21, 2007.

[30] A. Lali, A. Khare, J. Joshi, and K. Nigam, "Behaviour of solid particles in viscous non-Newtonian solutions: settling velocity, wall effects and bed expansion in solid-liquid fluidized beds," *Powder Technology,* vol. 57, pp. 39-50, 1989.

[31] R. Chhabra, M. Kumar, and R. Prasad, "Drag on spheres in rolling motion in inclined smooth tubes filled with incompressible liquids," *Powder technology,* vol. 113, pp. 114-118, 2000.

[32] V. C. Kelessidis, "Terminal velocity of solid spheres falling in Newtonian and non-Newtonian liquids," *Techn. Chron. Sci. J., Techn. Chamber Greece,* vol. 1, p. 2, 2003.

[33] V. C. Kelessidis, "An explicit equation for the terminal velocity of solid spheres falling in pseudoplastic liquids," *Chemical engineering science,* vol. 59, pp. 4437-4447, 2004.

[34] S. Dhole, R. Chhabra, and V. Eswaran, "Power law fluid flow through beds of spheres at intermediate reynolds numbers: Pressure in fixed and distended beds," *Chemical Engineering Research and Design,* vol. 82, pp. 642-652, 2004.

[35] P. Rajitha, R. Chhabra, N. Sabiri, and J. Comiti, "Drag on non-spherical particles in power law non-Newtonian media," *International Journal of Mineral Processing,* vol. 78, pp. 110-121, 2006.

[36] M. Renaud, E. Mauret, and R. P. Chhabra, "Power-law fluid flow over a sphere: Average shear rate and drag coefficient," *The Canadian Journal of Chemical Engineering,* vol. 82, pp. 1066-1070, 2004.

[37] A. Hazzab, A. Terfous, and A. Ghenaim, "Measurement and modeling of the settling velocity of isometric particles," *Powder Technology,* vol. 184, pp. 105-113, 2008.

[38] G. H. Ganser, "A rational approach to drag prediction of spherical and nonspherical particles," *Powder Technology,* vol. 77, pp. 143-152, 1993.

[39] J. A. Jiménez and O. S. Madsen, "A simple formula to estimate settling velocity of natural sediments," *Journal of waterway, port, coastal, and ocean engineering,* vol. 129, pp. 70-78, 2003.

[40] J. Valembois, "Direct Calculation of the Falling Speed of a Spherical Grain in a Fluid," *La Houille Blanche,* pp. 127-129, 1983.

[41] R. Turton and N. Clark, "An explicit relationship to predict spherical particle terminal velocity," *Powder Technology,* vol. 53, pp. 127-129, 1987.

[42] U. Ganguly, "On the prediction of terminal settling velocity of solids in liquid-solid systems," *International Journal of Mineral Processing,* vol. 29, pp. 235-247, 1990.

[43] L. Trim, K. She, and D. Pope, "Settling velocities of large natural sediments," in *Proc. 4th Conf. on HydroScience and Engineering, Seoul*, 2000.

[44] K. Tsakalakis and G. Stamboltzis, "Prediction of the settling velocity of irregularly shaped particles," *Minerals Engineering,* vol. 14, pp. 349-357, 2001.

[45] J. Gabitto and C. Tsouris, "Drag coefficient and settling velocity for particles of cylindrical shape," *Powder Technology,* vol. 183, pp. 314-322, 2008.

[46] A. Haider and O. Levenspiel, "Drag coefficient and terminal velocity of spherical and nonspherical particles," *Powder technology,* vol. 58, pp. 63-70, 1989.

[47] R. Chhabra, L. Agarwal, and N. K. Sinha, "Drag on non-spherical particles: an evaluation of

available methods," *Powder Technology*, vol. 101, pp. 288-295, 1999.

[48] B. Camenen, "Simple and general formula for the settling velocity of particles," *Journal of Hydraulic Engineering*, vol. 133, pp. 229-233, 2007.

[49] S. Morsi and A. Alexander, "An investigation of particle trajectories in two-phase flow systems," *Journal of Fluid mechanics*, vol. 55, pp. 193-208, 1972.

[50] P. D. Komar, "Settling velocities of circular cylinders at low Reynolds numbers," *The Journal of Geology*, vol. 88, pp. 327-336, 1980.

[51] R. Deigaard, *Mechanics of coastal sediment transport* vol. 3: World scientific publishing company, 1992.

[52] J. S. Serafini, "Impingement of water droplets on wedges and double-wedge airfoils at supersonic speeds," 1954.

[53] G. W. Govier and K. Aziz, *The flow of complex mixtures in pipes* vol. 469: Van Nostrand Reinhold New York, 1972.

[54] F. M. White and I. Corfield, *Viscous fluid flow* vol. 3: McGraw-Hill New York, 2006.

[55] S. Tran-Cong, M. Gay, and E. E. Michaelides, "Drag coefficients of irregularly shaped particles," *Powder Technology*, vol. 139, pp. 21-32, 2004.

[56] A. Hölzer and M. Sommerfeld, "New simple correlation formula for the drag coefficient of non-spherical particles," *Powder Technology*, vol. 184, pp. 361-365, 2008.

[57] H. K. Versteeg and W. Malalasekera, *An introduction to computational fluid dynamics: the finite volume method*: Pearson Education, 2007.

[58] ANSYS, "Fluent Theory and Guide," 2016.